IJE TRANSACTIONS C: Aspects Vol. 37 No. 06, (June 2024) 1183-1193

International Journal of Engineering

Journal Homepage: www.ije.ir

Using Reluctance Torque Theory in Spoke Type Permanent Magnet Vernier Motors to Increase Average Torque

A. Imanifar, H. Yaghobi*

Faculty of Electrical and Computer Engineering, Semnan University, Semnan, Iran

P A P E R I N F O

Paper history:
Received 21 December 2023
Received in revised form 03 January 2024
Accepted 20 January 2024

Keywords:
Average Torque
Finite-element-method
Spoke type Vernier Permanent-magnet Motor
Reluctance Permanent Magnet Vernier Motor

A B S T R A C T

Conventional energy sources like fossil fuels are no longer viable due to their limitations and environmental impact. The demand for cleaner, more efficient energy solutions has led to the development of electric machines with smaller volumes and higher output. The family of permanent magnet Vernier motors have high torque output at very low speeds while being very small in volume. In conventional SVPM, the core losses are high, which leads to heating and reducing the efficiency of the motor, and the power factor of the motor is also low, and the torque can increase in relation to the motor volume. The reluctance torque theory, along with the normal output torque of the motor, increases the final torque of the motor. In addition, the toothing of the rotor reduces the cross-sectional area and weight of the rotor. With the reduction of the cross-sectional area, the eddy currents in the core are reduced, the power factor increases and the efficiency of the motor improves. Therefore, in this paper, a spoke-type permanent magnet Vernier motor with a rotor similar to the reluctance rotor has been designed, which has higher torque, lower losses, and higher power factor compared to conventional spoke-type permanent magnet Vernier motors.

***doi**: 10.5829/ije.2024.37.06c.15*

Graphical Abstract

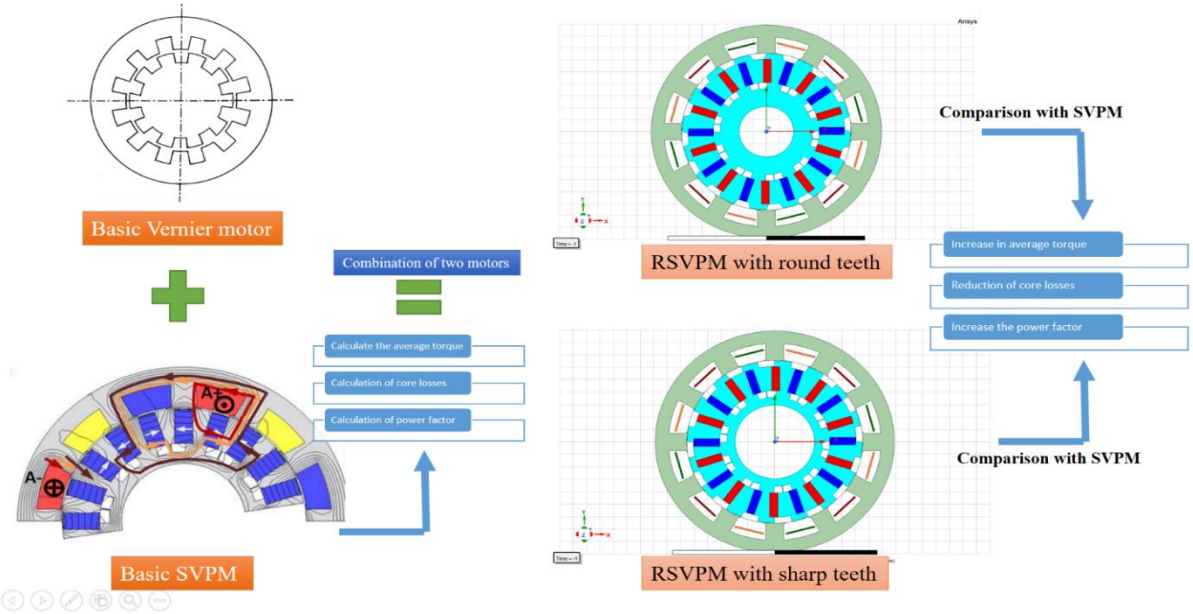

*Corresponding Author: Email: yaghobi@semnan.ac.ir (H. Yaghobi)

Please cite this article as: Imanifar A, Yaghobi H. Using Reluctance Torque Theory in Spoke Type Permanent Magnet Vernier Motors to Increase Average Torque. International Journal of Engineering, Transactions C: Aspects. 2024;37(06):1183-93.

1. INTRODUCTION

Permanent magnet motors are used in various industries such as electric traction, material forming, and electric vehicle industry (1). These motors are used in turbine systems due to their high efficiency and low maintenance costs (2). Economic reasons, cost competitiveness and availability of rare earth magnets are among the reasons that have made permanent magnet Vernier motors as well as permanent magnet motors important and widely used (3).

Rare earth magnets ultimately reduce the volume of the machine due to increased flux density compared to other magnets (4). Two kinds of interior PM (IPM) and surface mounted PM (SPM) machines are becoming candidates in high speed applications and Vernier machines are used in low speed applications (5). The shape of the placement of magnets in these motors has caused them to have various applications in the industry, of which the Halbach and spoke arrangement is one of the newest types (6). In other permanent magnet motors, in addition to the type of placement of magnets, the reluctance torque theory is used, which operates based on two different paths for the flux produced by the armature coil in the air gap (7).

The design of machine controlled with flux by high speed, as well as the design of the machine with low speed and high production torque, are very important and have many applications (8). The idea of the Vernier machine was first expressed in 1963 when it was proposed as a synchronous motor that has a reluctance model (9). The principle of operation of reluctance motors is the existence of non-uniform areas with low and high magnetic permeability between the stationary and moving parts of a motor. In the reluctance Vernier motor, the shape of the rotor and stator are made of teeth, and the number of teeth is not equal and slightly different. In these motors, in the areas where the stator teeth are aligned with the rotor teeth, the magnetic permanence is higher, and in the areas where the stator teeth are opposite to the rotor teeth, the magnetic permanence is lower (10). In 1995, a design was given that optimized Vernier motors, and in this design, a permanent magnet was used to increase the output torque density at the low speed (11). This design was named permanent magnet Vernier motors (PMVM).

Torque density has always been an important issue regarding Vernier machines (VM), which has been addressed over time by presenting different structures. These structures include the double rotor structures and the double excitation structure, which increase the torque density by increasing the area of the air gap (12-14).

High power factor is important in permanent magnet Vernier motors (PMVM) (15). A model for increasing the power factor is proposed by Li et al. (16). In this design, the magnets are placed in such a way that compared to the conventional permanent magnet Vernier motors, it has less air gap. In these motors, magnetic flux is used in such a way that it has a higher torque density than conventional models (17, 18).

The magnets used on the surface of the rotor of this motor are of the rare earth type, which is very expensive. Manufacturers can use cheaper magnets to reduce costs as reviewed by Du and Lipo (18). The permanent magnet Vernier motor that has been reviewed by Liu and Lipo (19) uses flux barriers, which causes high torque density to be produced.

In this paper, the permanent magnet Vernier motor will be discussed with the reluctance design on its rotor, which ultimately has a higher density and average torque than conventional permanent magnet Vernier motors. In this study, a permanent magnet Vernier machine with a flux barrier behind the magnet is designed and a reluctance scheme is implemented on it. In this design, the air gap between the rotor and the stator is non-uniform and the rotor is toothed. In this type of motor, in addition to the main torque that is produced, the reluctance torque caused by the rotor teeth will be created and will be added to the main torque of the machine.

2. OPERATION PRINCIPLE OF VERNIER MACHINE

The operation of the permanent magnet Vernier motor is similar to a gearbox. In gearboxes, the torque of the outer rotor is different from the torque of the inner rotor. In these motors, the frequency caused by the torque of the rotor is different from the frequency caused by rotation, and this property is similar to the operation of a gearbox (20), so to better understand how to produce torque in permanent magnet Vernier motors (PMVMs), studies on torque production in gearboxes carried out.

The family of Vernier machines is very diverse. The performance of each of them is different from each other and they have different applications in the industry. Figure 1 illustrates the geometry of a simple Vernier motor. This motor has a toothed stator and a toothed rotor. The geometry of this motor is similar to synchronous reluctance motors and its torque increases as the rotor speed decreases. The stator of this type of motor has open slots with uniform winding distribution similar to an induction motor.

The reluctance Vernier motor (RVM) that can be seen in Figure 2 has a toothed rotor and a toothed stator [10], and in some areas the magnetic permeability between the rotor and stator is maximum and in some areas, the magnetic permeability is minimum because the air gap between the rotor and stator is uniform. In these motors, sometimes the pitch of the stator slot is larger than the pitch of the rotor slot, and sometimes the pitch of the rotor slot is larger than the pitch of the stator slot. The torque production in RVM depends on the teeth, gaps,

and magnetomotive force waveform. The rotor speed of RVM is a fixed fraction of the rotation speed of the magnetomotive force waveform, which is constant and synchronous.

The permanent magnet Vernier motor shown in Figure 3 is another type of Vernier motor family that has a magnet placed on its rotor. The air gap between the rotor and the stator of these types of motors is uniform. In these motors, due to the presence of magnets on the rotor, the rotor torque density is higher and as a result, the output torque is higher. This motor has the same structure as the surface permanent magnet Vernier motor, and their difference is in the number of rotor poles and the winding, which has more rotor poles. This motor has similar teeth on the surface of the stator towards the air gap (12).

2. 1. Flux Barrier Design In permanent magnet Vernier machines, there is a virtual gearbox, which is suitable for low-speed, high-torque direct drive applications. Usually, the gear ratio of this virtual gearbox is p_r / p_s ; where p_r is the number of rotor poles

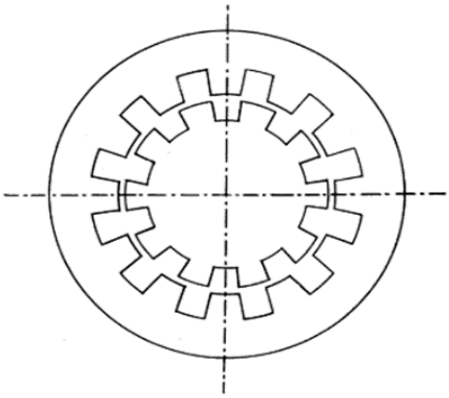

Figure 1. A simple Vernier motor (9)

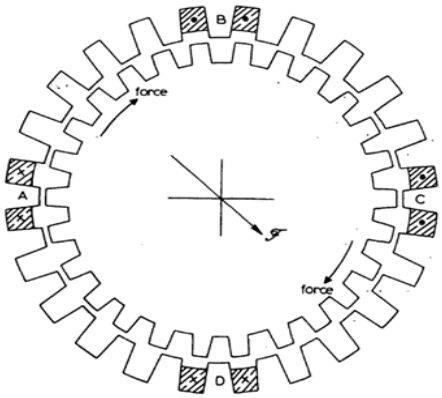

Figure 2. Reluctance Vernier motor (RVM) (10)

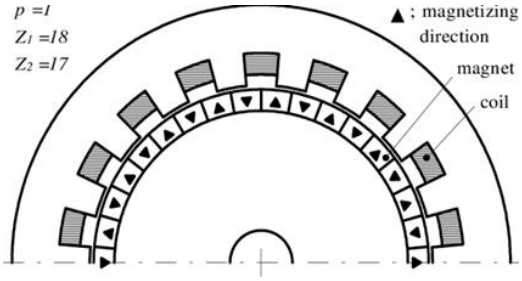

Figure 3. A simple permanent magnet Vernier machine (13)

and p_s is the number of stator poles. Figure 4 shows the design of a piecemeal flux barrier on the rotor of a permanent magnet Vernier machine, abbreviated as SVPM (17), is introduced. This type of flux barrier can maintain the power factor of the motor and simplify the production process of this type of motor for use in the industry.

Figure 5 shows unlike the previous case, the flux barriers are placed continuously. The number of these flux barriers under each pole is half of the case where the flux barriers are placed in pieces under each pole.

Flux barriers cause the magnetic flux to be locked in a specific path between the rotor and the stator. In the case where continuous flux barriers are used because the iron of the rotor is used less, the iron loss of the rotor is reduced, and this causes the heat of the rotor core to decrease during operation. Figure 6 shows the comparison result between the two cases mentioned above.

3. DESIGN RELATION OF PERMANENT MAGNET VERNIER MACHINE

In this section, the equations governing permanent magnet Vernier machines were discussed. These equations include torque theory in conventional

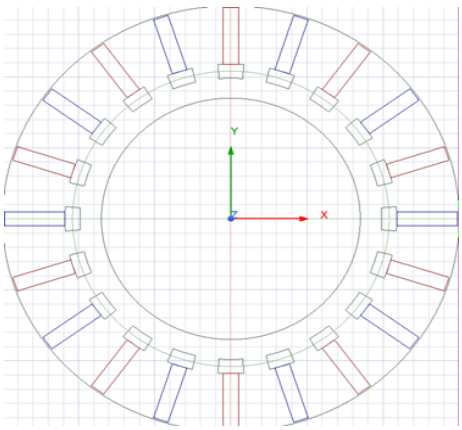

Figure 4. Topology of patchy flux barrier

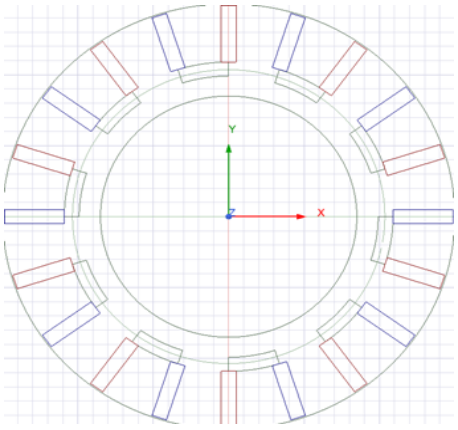

Figure 5. Topology of continuous flux barrier

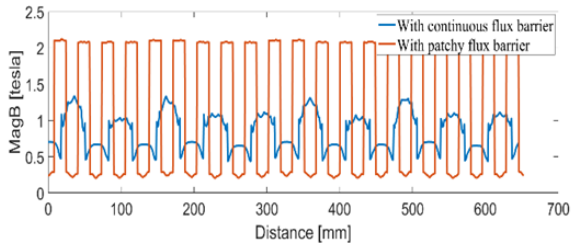

Figure 6. Comparison of the rotor magnetic flux density between the two states of continuous flux barrier and patchy flux barrier, which indicates the heat of the rotor

permanent magnet Vernier machines. The torque caused by the magnetic driving force is expressed, and then the torque caused by the magnetic flux is given, and after that, the theory of torque in permanent magnet Vernier machines is discussed.

3. 1. Design Equation In a permanent magnet Vernier machine, the number of slots on the stator is obtained as follows (11):

$$z_1 = 6pq \tag{1}$$

where p shows the number of stator poles and q shows the number of stator slots per phase. For as much as (11):

$$z_2 = z_1 + p \tag{2}$$

By inserting Equation 2 into Equation 1, the following equation is obtained (4).

$$z_2 = (1+6q)p \tag{3}$$

where the number of rotor slots is obtained. The three-phase current of the start winding is obtained according to Equation 4 (11).

$$i_{1h} = \sqrt{2} i_1 \cos(\omega t - (h-1)\frac{2\pi}{3}) \tag{4}$$

where the value h depends on the phase. This value is 1 for the first phase, 2 for the second phase, and 3 for the third phase. The magnetomotive force resulting from per phase is obtained from Equation 5 (11).

$$F_1 = \sum^{(-1)^q} \frac{3N_1 i_1 k_{w(1+6l)}}{\sqrt{2} p\pi(1+6l)} \times \cos((1+6l)p\theta_1 - \omega t) \tag{5}$$

Respectively, N_1, i_1, $k_{w(1+6l)}$, θ_1, ω are the number of conductors connected in series in the stator winding, the effective value of the stator current, the winding factor, spatial angle, and the frequency angle of the stator current.

Specific loading in permanent magnet machines is obtained as follows (11):

$$ac = \frac{3k_{w1}N_1 i_1}{\pi D} \tag{6}$$

where D is the inner diameter of the stator core. The polar pitch in permanent magnet Vernier machines is obtained from Equation 7 (11).

$$\tau = \frac{\pi D}{2p} \tag{7}$$

3. 2. The Torque Caused by The Magnetic Driving Force The magnetic driving force and the flux density are used to obtain the output torque, which is given in Equation 8 (11).

$$T = z_2 \times \frac{3\tau l_a N_1 i_1}{\sqrt{2}\pi} \times \left\{ k_{w1} B_{m1} + (-1)^q \frac{k_{w(1+6q)}}{1+6q} B_m (1+6q) \right\} \times \sin\{(\omega - z_2\omega_m)t + z_2\xi\phi_2\} \tag{8}$$

where l_a the length of the core and other parameters are introduced in the previous equations. Figure 7 shows the geometry of the $\xi\phi_2$.

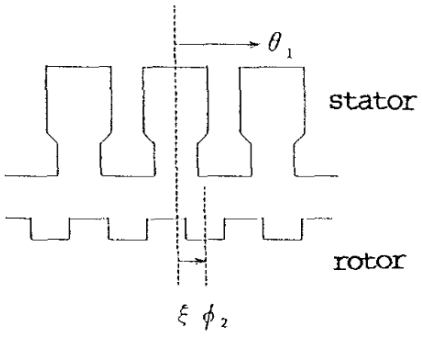

Figure 7. Geometric view of θ_1 and $\xi\phi_2$ on rotor and stator geometry of permanent magnet Vernier machine (11)

If the rotor moves at a constant speed, its angular is as follows (11).

$$\omega_m = \frac{\omega}{z_2} \tag{9}$$

The torque equation obtained in Equation 8 is written as Equation 9 (11).

$$T = z_2 \times \frac{3\tau l_a N_1 i_1}{\sqrt{2}\pi} \times \left\{ k_{w1} B_{m1} + (-1)^q \frac{k_{w(1+6q)}}{1+6q} B_m (1+6q) \right\} \times \sin\{z_2 \xi \phi_2\} \tag{10}$$

There is a sinusoidal expression in Equation 10. So the maximum and minimum torque values can be calculated. The maximum and minimum values are respectively at $\xi\phi_2 = \pm \pi/2$ because the sinusoidal expression is placed between its minimum and maximum values at these points.

3. 3. Torque Due to Magnetic Flux The magnetic flux caused by the magnet on the rotor produces torque. The maximum torque produced due to this flux is obtained from Equation 11 (11).

$$T_{vm1} = z_2 \times \frac{3\tau l_a N_1 i_1}{\sqrt{2}\pi} k_{w1} B_{m1} \tag{11}$$

3. 4. Torque Theory in SVPM In SPVM, magnets on the surface of the rotor use flux barriers, which are called flux barriers because of the use of these flux barriers. In these machines, the magnetic flux closes its path in such a way that it can perform better in torque production and ultimately produce better torque compared to conventional permanent magnet Vernier machines.

The magnets on the rotor may be placed on the surface of the rotor or buried in the rotor, depending on the type of application in the industry. Figure 8 shows a view of the SPVM, with a piecemeal flux barrier placed on the rotor and behind the magnets.

The spatial angle of the rotor magnets in the SPVM is as follows (18).

$$\theta_r = \theta_s - \theta_{rm} \tag{12}$$

where the spatial angle of the MMF stator θ_r and spatial angle of the rotor magnet θ_s and mechanical rotor rotation angle θ_{rm}. In the air gap of SPVM, the flux density is calculated through Equation 13 (18).

$$B_{rg} = \hat{P}(\theta) B_g(\theta_s) \tag{13}$$

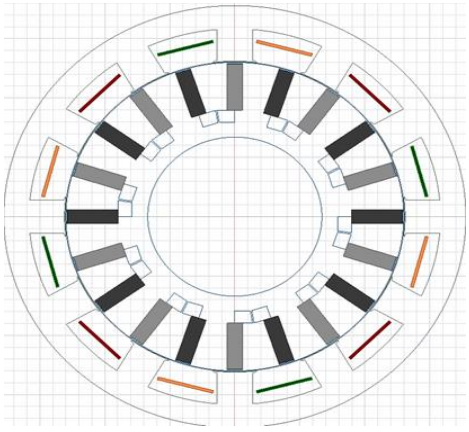

Figure 1. A view of the SPVM with flux barrier

where the magnetic permeability $\hat{P}(\theta)$ and the air gap flux density $B_g(\theta_s)$ modulated by the stator teeth. Finally, the torque in SVPM is obtained from Equation 14 (11).

$$T = \frac{d_{is} l_i}{2} \int_0^{2\pi} \left(\frac{\partial}{\partial \theta_{rm}} B_{rg} \right) F_{sg} \, d\theta_s \tag{14}$$

where the magnetic driving force F_{sg} by the permanent magnets on the rotor.

4. THE PROPOSED RELUCTANCE SPOKE TYPE PERMANENT MAGNET VERNIER MACHINE

Nowadays, motors with low heat losses, low noise, low weight, and low iron losses are highly regarded (21). Conventional SVPMs have a simple circular rotor. In this research, the idea of a reluctance motor is taken. The basis of reluctance motors is the theory of reluctance torque, which is made by a non-uniform and toothed rotor. In this paper, a non-uniform and toothed rotor is designed for conventional spoke-type permanent magnet motors, the resulting reluctance torque comes with the help of the main torque of the motor and increases the average torque produced from its conventional state. Du and Lipo (18) simulated a conventional spoke-type permanent magnet Vernier motor. The stator of this motor has 4 poles and its rotor has 20 poles, and the motor excitation frequency is 66.67 Hz. The average torque produced by this motor is around 605 Nm. The idea of this paper is implemented on this motor, and it is designed in a non-uniform and toothed way so that the reluctance torque increases the average torque produced by this motor. In other words, the motor designed in this paper is a new type of SVPM in which reluctance torque is used, which is an RSVPM (Reluctance Spoke Type Permanent Magnet Vernier motor). Equation 15

generally obtained the method of calculating the core losses in an electric machine.

$$P_{core} = KB^2 f n_f s f_{loss} \quad (15)$$

In Equation 15, with decreasing cross-section (s), the losses decrease. Therefore, toothing the rotor reduces core losses. On the other hand, the core leakage factor (f_{loss}) also decreases significantly because with toothing the rotor, the magnetic field around the rotor is cut off and fewer eddy currents flow in the core. Therefore, by reducing the weight and core leakage factor, core losses are greatly reduced and the efficiency of the motor is increased.

4. 1. Equation of Number of Rotor Teeth

According to Equation 2, the number of rotor teeth can be calculated. To calculate the number of rotor teeth, the number of stator slots must be calculated first. In an SVPM, the number of stator slots is calculated from Equation 16 (18):

$$S_s = 3Pq \quad (16)$$

where P is the number of poles of the rotating magnetic field and q is a quantity related to the winding factor, which is 1 for the type of winding. Therefore, by substituting Equation 16 into Equation 2, the following equation is calculated, which shows the number of rotor teeth:

$$Z_2 = (3Pq) + P = P(3q + 1) \quad (17)$$

The number of stator poles is 4. According to Equation 16, the number of stator teeth is 12 and According to Equation 17, the number of rotor teeth is 16.

4. 2. Finite Element Method Analysis

In this section, computer simulation in Ansys Electronics software is presented in two dimensions. Maxwell software can analyze the target motor in transient mode (22, 23). In Figure 9 the rotor teeth are designed as sharp teeth.

In Figure 10 the rotor is designed as a toothed rotor with round teeth.

For RSVPM, the simulation is done for two types of rotors designed separately and the torque results are reported. The motor design parameters are listed in Table 1.

The parameters shown in the SVPM in Figure 11 are similar to the RSVPM, and only its rotor is toothed. The geometry model of the first simulation of RSVPM is shown in Figure 12 and the rotor teeth are sharp in this simulation.

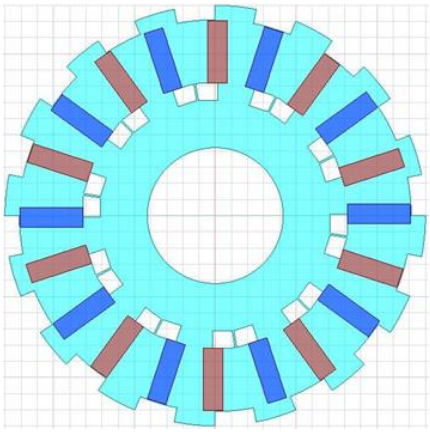

Figure 9. A view of the rotor with sharp teeth in the RSVPM

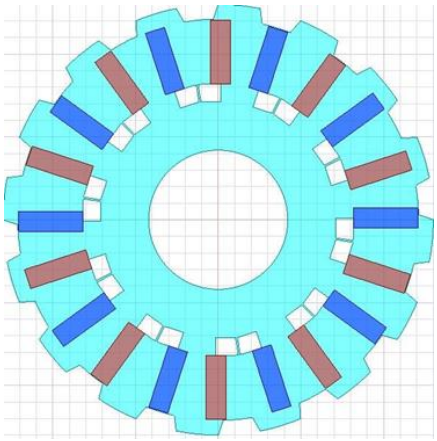

Figure 10. A view of the rotor with round teeth in the RSVPM

TABLE 1. Design Key Dimensions

Parameters	Conventional SVPM [19]	Proposed RSVPM
Stator OD/ID [mm]	355.6/261.7	360/262
Rotor OD/ID [mm]	259.7/133	260/84
D_{cs} [mm]	19.8	19.8
D_{cr} [mm]	13.5	13.5
τ_s [°]	30	30
τ_{pr} [°]	18	18
d_{pm}/w_{pm} [mm]	20.8/38.9	20.8/38.9
d_{bg1}/d_{bg2} [mm]	0.5/0.8	0.5/0.8
d_b/w_b [mm]	14.6/10.4	14.6/10.4
Number of rotor teeth	-	16

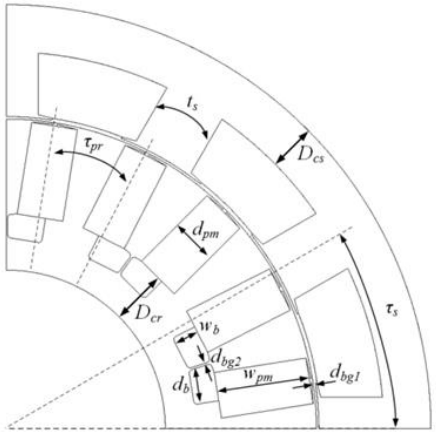

Figure 11. The parameters used in the geometry of the SVPM (19)

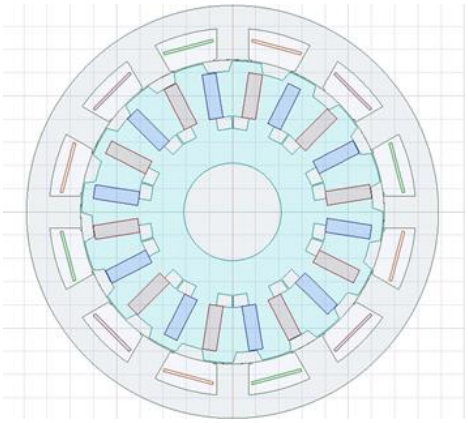

Figure 12. A view of the RSVPM with round teeth

The simulation done by the finite element analysis method is for the round tooth RSVPM. The average motor torque is shown in Figure 13.

The average torque of this motor is 931.8 Nm. Core losses are also shown in Figure 14.

The average loss of the rotor core is 128.31 W. Core losses are higher in conventional SVPM. By analyzing

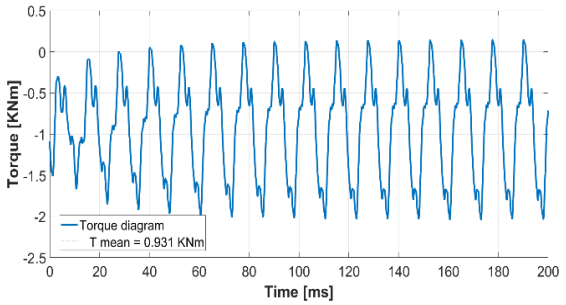

Figure 13. RSVPM torque diagram and the average value of the produced torque with a round-toothed rotor

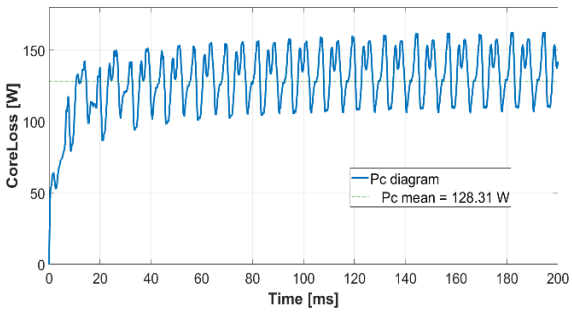

Figure 14. RSVPM core loss diagram with a round-toothed rotor

the simulation and drawing the core loss diagram in Figure 15, the average value of core loss in SVPM is obtained.

The back EMF diagram for three phases of the proposed RSVPM is shown in Figure 16.

The maximum voltage value in phase A is 283.4 V, in phase B is 281.9 V, and in phase c is 282.2 V. The direction of movement of magnetic flux lines and distribution of flux density is shown in Figure 17.

Now the second design is done for RSVPM with sharp teeth. The result of the finite element method for this motor is reported. The average torque produced by this motor is given in Figure 18.

The diagram of core losses in the RSVPM with sharp teeth is shown in Figure 19. It can be seen that the core

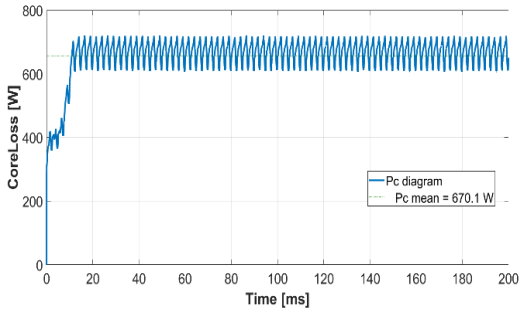

Figure 15. Core losses in conventional SVPM [18]

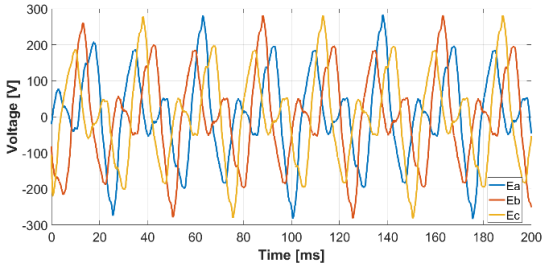

Figure 16. RSVPM back EMF diagram with a round-toothed rotor

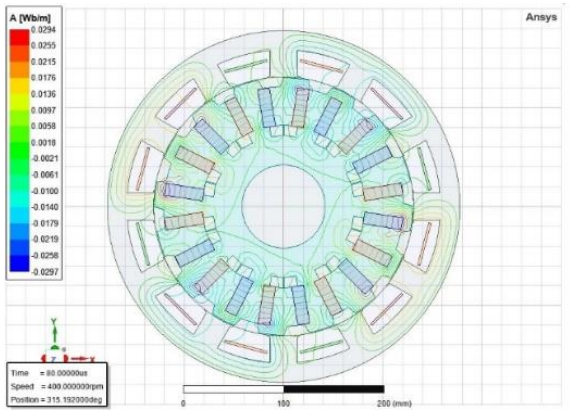

(a)

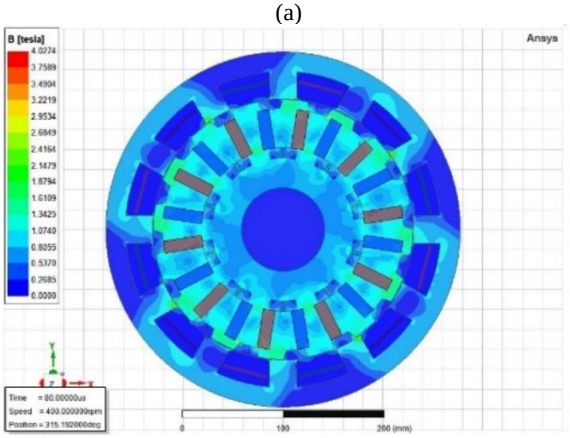

(b)

Figure 17. The RSVPM with round teeth. (a) The path of the flux lines. (b) Distribution of flux density

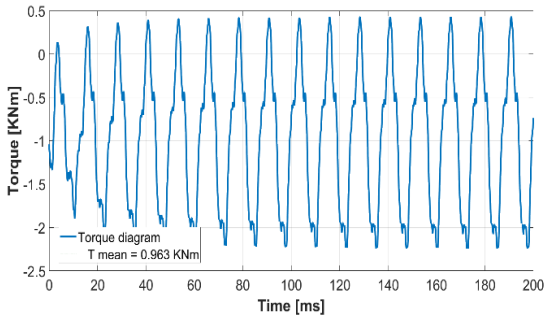

Figure 18. Torque diagram of an RSVPM with sharp teeth

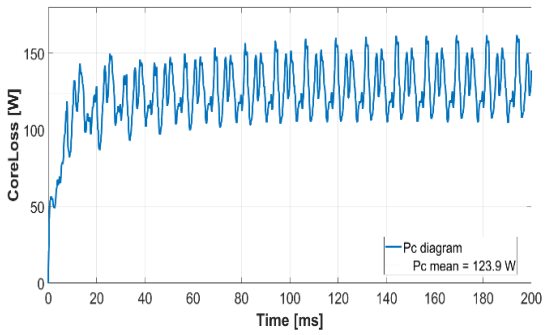

Figure 19. Core losses in RSPVM with sharp teeth

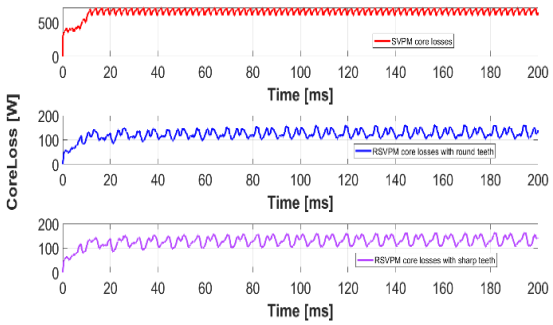

Figure 20. Comparison of core losses of RSVPM and SVPM

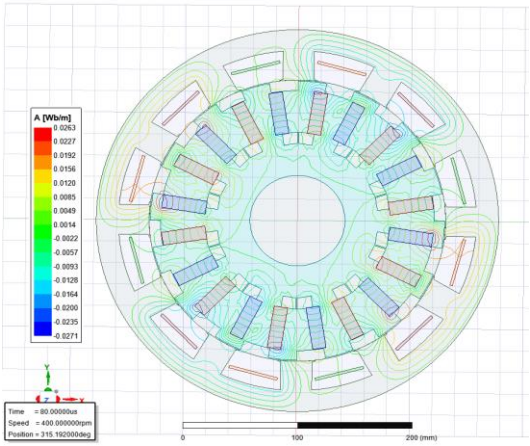

Figure 21. The path of flux lines in RSVPM with sharp teeth

loss in this motor is less than that of conventional SVPM and it is almost the same compared to RSVPM with round teeth. The large difference in core losses between the RSVPM and the conventional SVPM is seen in Figure 20, which are compared to each other.

The path of flux lines in RSVPM with sharp teeth is shown in Figure 21. In Figure 22, the distribution of the magnetic flux density of the motor is also done, which shows that the motor does not reach saturation at any point.

To calculate the power factor, the voltage and current diagrams of the motor are drawn in a coordinate plane (24). The horizontal axis of time is common to both graphs in the coordinate plane. Then, in the selected cycle, the times when the voltage and current become zero are extracted and multiplied by the motor excitation frequency. The angle between voltage and current is calculated using this technique. Then, through the cosine between the angle of voltage and current in that cycle, the power factor of the motor can be calculated. The power

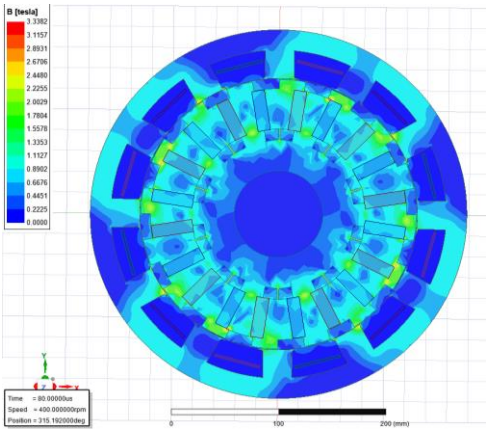

Figure 22. Distribution of flux density in the RSVPM with sharp teeth

factor in conventional SVPM is 0.62. According to Figure 23, which is obtained from the software simulation, it can calculate the value of the power factor for the RSVPM with sharp teeth.

$$\phi_{RSVPM}^{sharp} = \frac{m_1 - m_2}{\frac{1}{f_{ex}}} = \frac{4.9997 - 6.9328}{\frac{1}{66.67}} = -132.1799^{\circ}$$

$$PF_{RSVPM}^{sharp} = \cos(\phi) = \cos(-132.1799) = -0.6715$$

According to Figure 24, which is obtained from the software simulation, it can calculate the value of the power factor for the RSVPM with round teeth.

$$\phi_{RSVPM}^{round} = \frac{m_1 - m_2}{\frac{1}{f_{ex}}} = \frac{4.9998 - 7.2914}{\frac{1}{66.67}} = -152.7810^{\circ}$$

$$PF_{RSVPM}^{round} = \cos(\phi) = \cos(-152.7810) = -0.8893$$

To calculate the efficiency, the output power must be calculated. With the help of Equations 18 and 19, the efficiency can be calculated.

$$P_{out} = \frac{T_m . N_m}{9.5488} \tag{18}$$

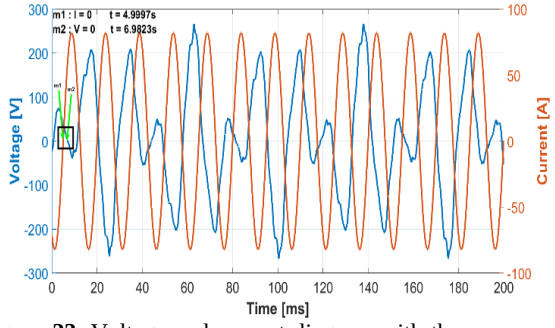

Figure 23. Voltage and current diagram with the common time axis in the RSVPM with sharp teeth

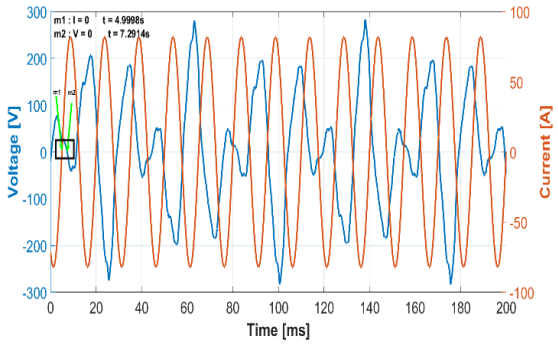

Figure 24. Voltage and current diagram with the common time axis in the RSVPM with round teeth

$$\eta = \frac{P_{out}}{P_{out} + P_{fe} + P_{cu}} \tag{19}$$

where the average torque T_m, the rotor speed N_m, the output power P_{out}, core loss P_{fe}, copper loss P_{cu} and efficiency η. According to the excitation frequency and the number of rotor poles, the rotor speed is 400 rpm. Through the simulations, the values of core loss, copper loss, and average torque have been calculated for sharp tooth and round tooth rotors. Therefore, the amount of return can be calculated for each.

$$P_{out}^{RSVPM\_sharp} = \frac{963N.m \times 400rpm}{9.5488} = 40340.147W$$

$$\eta_{RSVPM}^{sharp} = \frac{40340.147}{40340.147 + 123.9 + 979.16} = 0.9734$$

$$P_{out}^{RSVPM\_round} = \frac{931N.m \times 400rpm}{9.5488} = 38999.664W$$

$$\eta_{RSVPM}^{round} = \frac{38999.664}{38999.664 + 128.3 + 979.16} = 0.9724$$

According to the calculations, the efficiency in the case of the rotor with round teeth is 97.24%, and in the case of the rotor with sharp teeth 97.34%.

Table 2 shows a comparison between the RSVPM with sharp teeth the RSVPM with round teeth and the conventional SVPM.

TABLE 2. Parameters and Performance Comparison

	Proposed RSVM with round teeth	**Conventional SVPM [18]**	**Proposed RSVPM with sharp teeth**
Machine type	**VPM**	**VPM**	**VPM**
Magnet type	NdFeB/1.2	NdFeB/1.2	NdFeB/1.2

SSP	1	1	1
Stator/rotor pole number	4/20	4/20	4/20
Stator OD [mm]	355.5	360	355.5
Stack length [mm]	311	311	311
Excitation frequency [Hz]	66.67	66.67	66.67
Power factor	0.88	0.62	0.67
Torque [Nm]	931	605	963
Core loss [W]	128.3	671.3	123.9

5. CONCLUSIONS

In this paper, permanent magnet motors were investigated. First, the conventional spoke-type permanent magnet Vernier motor (SVPM) was checked and from the simulation, it was concluded that the average torque produced by this motor is 605 Nm and the core loss of the rotor is 671 watts. Then two types of rotors are designed using the reluctance torque theory, in the first case, the rotor with sharp teeth, and it was observed that in this case, the average torque produced is about 963 Nm, which has improved by about 59% and the core loss of rotor is about 124 watts, which has improved by about 81% compared to the conventional SVPM, and this makes the rotor core cooler while working. This issue can be seen in the monitoring of the magnetic flux density distribution of the motor, In the second case, the rotor with round teeth, it was observed that in this case, the average torque produced is 931 Nm, which is about 53% better compared to the conventional SVPM, and of course compared to the sharp tooth type it has a lower average torque, but the advantage of a round tooth over a sharp tooth is that it has a lower torque ripple. Also, in the round tooth type, the core loss of the rotor is almost 128 watts, which is 81% better compared to the conventional SVPM and it is almost no difference compared to the sharp tooth type. Regarding the power factor, the power factor has increased by 8.06% in RSVPM with sharp-toothed rotors, and the power factor has increased by 41.94% in RSVPM with round-toothed rotors.

6. REFERENCES

1. Gherabi Z, Toumi D, Benouzza N, Bendiabdellah A. A proposed approach for separation between short circuit fault, magnetic saturation phenomenon and supply unbalance in permanent magnet synchronous motor. International Journal of Engineering, Transactions A: Basics. 2020;33(10):1968-77. 10.5829/IJE.2020.33.10A.15
2. Karimpour S, Besmi M, Mirimani S. Multi-objective optimization design and Verification of Interior PMSG Based on Finite Element Analysis and Taguchi method. International Journal of Engineering, Transactions C: Aspects. 2021;34(9):2097-106. https://doi.org/10.5829/IJE.2021.34.09C.07
3. Parivar H, Seyyedbarzegar S, Darabi A. An improvement on slot configuration structure of a low-speed surface-mounted permanent magnet synchronous generator with a wound cable winding. International Journal of Engineering, Transactions C: Aspects. 2021;34(9):2045-52. 10.5829/ije.2021.34.09c.01
4. Patel A, Suthar B. Cogging torque reduction of sandwiched stator axial flux permanent magnet brushless dc motor using magnet notching technique. International Journal of Engineering, Transactions A: Basics. 2019;32(7):940-6. 10.5829/ije.2019.32.07a.06
5. Parivar H, Darabi A. Design and Modeling of a High-Speed Permanent Magnet Synchronous Generator with a Retention Sleeve of Rotor. International Journal of Engineering, Transactions B: Applications. 2021;34(11):2433-41. 10.5829/IJE.2021.34.11B.07
6. Song N, Zhu M, Zhou G, Guo L, Mu Y, Gao J, et al. Design and optimization of halbach permanent magnet array with rectangle section and trapezoid section. International Journal of Engineering, Transactions B: Applications. 2021;34(11):2379-86. 10.5829/IJE.2021.34.11B.01
7. Aghazadeh H, Afjei E, Siadatan A. Comprehensive design procedure and manufacturing of permanent magnet assisted synchronous reluctance motor. International Journal of Engineering, Transactions C: Aspects,. 2019;32(9):1299-305. https://doi.org/10.5829/ije.2019.32.09c.10
8. Liu C, Zhong J, Chau K. A novel flux-controllable vernier permanent-magnet machine. IEEE Transactions on Magnetics. 2011;47(10):4238-41. https://doi.org/10.1109/TMAG.2011.2152374
9. Lee C. Vernier motor and its design. IEEE Transactions on Power Apparatus and Systems. 1963;82(66):343-9. https://doi.org/10.1109/TPAS.1963.291362
10. Mukherji K, Tustin A, editors. Vernier reluctance motor. Proceedings of the Institution of Electrical Engineers; 1974: IET.
11. Ishizaki A, Tanaka T, Takasaki K, Nishikata S, editors. Theory and optimum design of PM Vernier motor. 1995 Seventh International Conference on Electrical Machines and Drives (Conf Publ No 412); 1995: IET.
12. Toba A, Lipo TA, editors. Novel dual-excitation permanent magnet vernier machine. Conference Record of the 1999 IEEE Industry Applications Conference Thirty-Forth IAS Annual Meeting (Cat No 99CH36370); 1999: IEEE.
13. Toba A, Lipo TA. Generic torque-maximizing design methodology of surface permanent-magnet vernier machine. IEEE transactions on industry applications. 2000;36(6):1539-46. https://doi.org/10.1109/28.887204
14. S. Niu, Ho SL, Fu WN, Wang LL. Quantitative Comparison of Novel Vernier Permanent Magnet Machines. IEEE Transactions on Magnetics. 2010;46:2032–5. https://doi.org/10.1109/28.887204
15. Arish N, Teymoori V. Development of linear vernier hybrid permanent magnet machine for wave energy converter. International Journal of Engineering, Transactions B: Applications. 2020;33(5):805-13. https://doi.org/10.5829/ije.2020.33.05b.12
16. Li D, Qu R, Lipo TA. High-power-factor vernier permanent-magnet machines. IEEE transactions on industry applications. 2014;50(6):3664-74. https://doi.org/10.1109/TIA.2014.2315443

17. Kim B, Lipo TA. Analysis of a PM vernier motor with spoke structure. IEEE Transactions on Industry Applications. 2015;52(1):217-25. https://doi.org/10.1109/TIA.2015.2477798
18. Du ZS, Lipo TA, editors. High torque density ferrite permanent magnet vernier motor analysis and design with demagnetization consideration. 2015 IEEE Energy Conversion Congress and Exposition (ECCE); 2015: IEEE.
19. Liu W, Lipo TA, editors. A family of vernier permanent magnet machines utilizing an alternating rotor leakage flux blocking design. 2017 IEEE energy conversion congress and exposition (ECCE); 2017: IEEE.
20. Liu W, Lipo TA, editors. Alternating flux barrier design of vernier ferrite magnet machine having high torque density. 2017 IEEE electric ship technologies symposium (ESTS); 2017: IEEE.
21. Siadatan A, Ghasemi S, Shamsabad Farahani S. Design and Construction of a Sensorless Circuit for Brushless DC Motor using Third Harmonic back Electromotive Force. International Journal of Engineering, Transactions A: Basics. 2017;30(4):500-6. 10.5829/idosi.ije.2017.30.04a.07
22. Arish N, Yaghobi H. Analysis of a New Linear Dual Stator Consequent Pole Halbach Array Flux Reversal Machine. International Journal of Engineering, Transactions B: Applications. 2021;34(8):2002-9. 10.5829/ije.2021.34.08b.21
23. Ardestani M, Arish N, Yaghobi H. A new HTS dual stator linear permanent magnet Vernier machine with Halbach array for wave energy conversion. Physica C: Superconductivity and its Applications. 2020;569:1353593. 10.1016/j.physc.2019.1353593
24. Xu L, Zhao W, Liu G, Song C. Design optimization of a spoke-type permanent-magnet vernier machine for torque density and power factor improvement. IEEE Transactions on Vehicular Technology. 2019;68(4):3446-56. https://doi.org/10.1109/TVT.2019.2902729

Persian Abstract

چکیده

منابع انرژی متعارف مانند سوخت های فسیلی به دلیل محدودیت ها و اثرات زیست محیطی دیگر قابل دوام نیستند. تقاضا برای راه حل های انرژی پاک تر و کارآمدتر منجر به توسعه ماشین های الکتریکی با حجم کمتر و خروجی بیشتر شده است. خانواده موتورهای ورنیه آهنربای دائمی دارای گشتاور خروجی بالا در سرعت های بسیار کم هستند در حالی که حجم بسیار کمی دارند. تئوری گشتاور رلوکتانسی همراه با گشتاور خروجی معمولی موتور، گشتاور نهایی موتور را افزایش می دهد. علاوه بر این، دندانه دار شدن روتور باعث کاهش سطح مقطع و وزن روتور می شود. با کاهش سطح مقطع، جریان های گردابی در هسته کاهش می یابد، ضریب قدرت افزایش می یابد و راندمان موتور بهبود می یابد. از این رو در این مقاله موتور ورنیر آهنربای دائم اسپوک با روتوری مشابه روتور رلوکتانسی طراحی شده است که در مقایسه با موتورهای ورنیر آهنربای دائمی معمولی دارای گشتاور بیشتر، تلفات کمتر و ضریب توان بالاتر است.